ELSEVIER

Journal of Nuclear Materials 218 (1994) 8–17

journal of nuclear materials

Revised formulae for sputtering data

C. García-Rosales, W. Eckstein, J. Roth

Max-Planck-Institut für Plasmaphysik, Euratom Association, Boltzmannstrasse 2, 85748 Garching bei München, Germany

Received 30 May 1994; accepted 30 August 1994

Abstract

A revision and improvement of analytic formulae for calculating sputtering yields is performed based on the large number of experimental and calculated sputtering yield data accumulated at IPP in the last three decades. The Bohdansky formula for calculating sputtering yields as a function of energy is revised by introducing a nuclear stopping cross-section based on an analytic fit to the Kr–C potential. New analytic expressions for the two fit parameters Q and E_{th} of the Bohdansky formula are deduced. Yamamura's formula for the angular dependence of the sputtering yield is shown not to be valid for self-sputtering and for heavy projectiles at energies near the threshold.

1. Introduction

One of the most critical problems in controlled thermonuclear fusion research is the erosion at limiters, divertor plates and vessel walls due to the impact of energetic plasma particles. This erosion causes a loss of material leading to thinning of the wall and to plasma contamination.

An important erosion process is physical sputtering, i.e. the removal of surface atoms from a solid due to the impact on energetic particles. The sputtering process can be described as a momentum transport in a collision cascade initiated by the incident particle in the surface layer of the solid. A surface atom is ejected if its energy is higher than the surface binding energy [1]. Physical sputtering is quantified by the sputtering yield Y defined as the mean number of atoms removed from the surface of a solid per incident ion.

The most widely used analytical formula for calculating sputtering yields was introduced in 1984 by Bohdansky [2]. The Bohdansky formula, which is based on Sigmund's analytic sputtering theory [1], describes the sputtering yield as a function of the projectile energy at normal incidence ($\alpha = 0°$)

$$Y(E_0, \alpha = 0°) = Q s_n^{TF}(\varepsilon)\left(1 - \left(\frac{E_{th}}{E_0}\right)^{2/3}\right)\left(1 - \frac{E_{th}}{E_0}\right)^2, \tag{1}$$

where E_0 is the projectile energy, α the angle of incidence, $s_n^{TF}(\varepsilon)$ the nuclear stopping cross section, and ε the reduced energy

$$\varepsilon = E_0 \frac{M_2}{M_1 + M_2} \frac{a_L}{Z_1 Z_2 e^2} = E_0 / E_{TF} \quad \text{with} \quad E_{TF} = \frac{Z_1 Z_2 e^2}{a_L} \frac{M_1 + M_2}{M_2}. \tag{2}$$

Z_1 and Z_2 are the nuclear charges, and M_1 and M_2 the masses of the projectile and the target atom, respectively. e is the electron charge ($e^2 = 14.4$ eV Å). The Lindhard screening length a_L is given by

$$a_L = \left(\frac{9\pi^2}{128}\right)^{1/3} a_B \left(Z_1^{2/3} + Z_2^{2/3}\right)^{-1/2} = 0.4685 \left(Z_1^{2/3} + Z_2^{2/3}\right)^{-1/2} \text{ Å}, \tag{3}$$

SSDI 0022-3115(94)00376-9

where a_B is the Bohr radius. The energy E_{TF} can be written

$$E_{TF}(\text{eV}) = 30.74 \frac{M_1 + M_2}{M_2} Z_1 Z_2 \left(Z_1^{2/3} + Z_2^{2/3}\right)^{1/2}. \tag{4}$$

The values Q and E_{th} in Eq. (1) are used as parameters to fit the sputtering data. Q determines the maximum of the yield curve, and E_{th} is the threshold energy where the sputtering yield becomes zero. The last two terms in Eq. (1) describe the threshold behaviour of the yield, not given in the analytic theory.

For the dependence of the sputtering yield on the angle of incidence of the bombarding particles, Yamamura [18] proposed a procedure which is based on the assumption that the angular dependence can be described by a factor to the yield at normal incidence

$$Y(E_0, \alpha) = Y(E_0, \alpha = 0°)(\cos \alpha)^{-f} \exp\left(f\left[1 - (\cos \alpha)^{-1}\right] \cos \alpha_{opt}\right). \tag{5}$$

The $(\cos \alpha)^{-f}$ term was proposed by Sigmund [1], the exponential term is chosen to produce a maximum in the angular dependence. The values f and α_{opt} are used as fitting parameters, where α_{opt} is the angle which corresponds to the maximum of the sputtering yield.

In a recent IPP report [4] we collected a large number of experimental and calculated yield data which include the experimental data compiled in an earlier report [5] and data accumulated in the years thereafter. During this compilation we found some systematic deviations of the data from the Bohdansky and Yamamura formulae which were the reason to think about possible improvements of Eqs. (1) and (5). For the case of the Bohdansky formula one point is that the nuclear stopping cross section $s_n^{TF}(\varepsilon)$ used in Eq. (1) is based on an analytic fit to the Thomas–Fermi potential [6,7] given by Matsunami et al. [8]. It is known that this cross-section is too large at low energies ($\epsilon < 0.01$). The other point is that values calculated with the Monte Carlo program TRIM.SP [9] using the Kr–C potential [10] are in good agreement with experimental data in many cases. Therefore, it seems reasonable to find a new fit for the stopping cross section s_n in Eq. (1) based on the Kr–C potential for a consistent fit of the calculated data with the Bohdansky formula (1). Finally, it would be of interest to find an analytic expression for the fit parameters Q and E_{th} in Eq. (1).

For the case of the Yamamura formula it was found during the compilation mentioned above that Yamamura's assumption of Eq. (5) is not correct in some cases. Yamamura gave also analytic scaling laws for calculating the fitting parameters f and α_{opt} of Eq. (5). However, these scaling laws are based on a relatively limited number of sputtering yield data. Due to the large number of data accumulated also for oblique angles of incidence it is possible to prove the validity of the formulae for f and α_{opt}.

2. New formulae for the energy dependence of the sputtering yield at normal incidence

The first step for a possible improvement of the Bohdansky formula is to replace the analytic fit to the Thomas–Fermi nuclear stopping cross section s_n^{TF} [8]

$$s_n^{TF}(\varepsilon) = \frac{3.441\sqrt{\varepsilon}\ln(\varepsilon + 2.718)}{1 + 6.355\sqrt{\varepsilon} + \varepsilon\left(6.882\sqrt{\varepsilon} - 1.708\right)}, \tag{6}$$

by one based on the Kr–C potential [10]. This stopping cross section s_n^{KrC} can be approximated by

$$s_n^{KrC}(\varepsilon) = \frac{0.5\ln(1 + 1.2288\varepsilon)}{\varepsilon + 0.1728\sqrt{\varepsilon} + 0.008\varepsilon^{0.1504}}. \tag{7}$$

Eq. (7) does not show the correct behaviour for high energies, as $s_n(\varepsilon)$ has to tend to $(\ln \varepsilon/\varepsilon)$ [11], but Eq. (6) with other constants does not reproduce the stopping determined from the Kr–C potential. In the energy range of interest ($\epsilon < 100$) Eq. (7) is a good approximation. The differences between the two equations for the nuclear stopping cross section (6) and (7) are shown in Fig. 1; the differences increase below $\varepsilon = 0.1$ down to lower reduced energies. The case of tungsten self-sputtering, see Fig. 2, demonstrates the better fit with the revised Bohdansky formula

$$Y(E_0, \alpha = 0°) = Q s_n^{KrC}(\varepsilon)\left(1 - \left(\frac{E_{th}}{E_0}\right)^{2/3}\right)\left(1 - \frac{E_{th}}{E_0}\right)^2, \tag{8}$$

which includes the new stopping cross-section formula (7). This revised Bohdansky formula (8) gives better agreement with experimental and calculated data than the original Bohdansky formula (1) but still exhibits

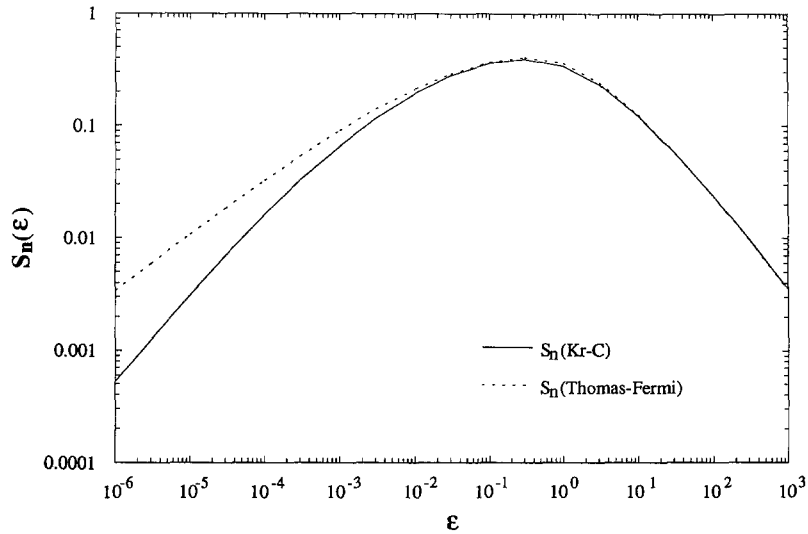

Fig. 1. Nuclear stopping cross section $s_n(\varepsilon)$ based on the Kr–C potential (solid line, calculated with Eq. (7)) and on the Thomas–Fermi potential (dashed line, calculated with Eq. (6)) as a function of the reduced energy ε.

deviations in the high keV range. Besides, the best fit to the data in the low keV range differs from calculated data in the energy regime near the threshold, see Fig. 2. Bohdansky [12] made an attempt to describe the behaviour of the threshold energy as a function of the mass ratio by the following formulae

$$E_{th} = \begin{cases} \dfrac{E_s}{\gamma(1-\gamma)} & \text{for} \quad \dfrac{M_1}{M_2} < 0.2, \\ 8E_s\left(\dfrac{M_1}{M_2}\right)^{2/5} & \text{for} \quad \dfrac{M_1}{M_2} > 0.2, \end{cases} \tag{9}$$

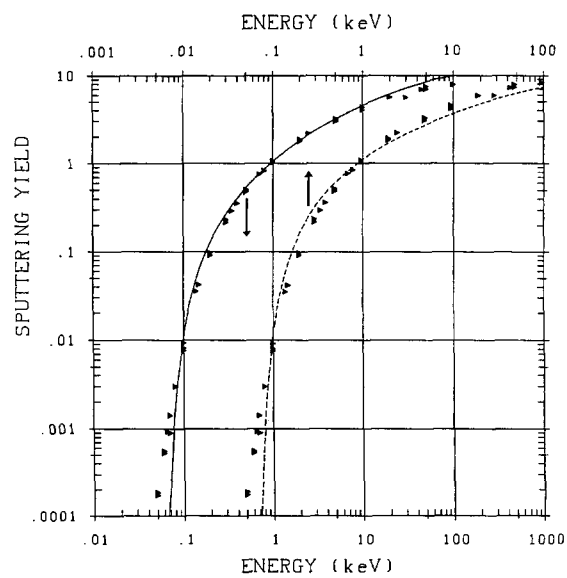

Fig. 2. Energy dependence of the tungsten self-sputtering yield fitted with the Bohdansky formula (1) (dashed line) and with the revised Bohdansky formula (8) (solid line).

where γ is the maximum energy transfer factor, $\gamma = 4M_1M_2/(M_1+M_2)^2$ and E_s is the surface binding energy (heat of sublimation). However, there exists a number of calculated data below the threshold energy given by Eq. (9). Taking these values into account for fitting with Eq. (8) leads to deviations of the fit with the available data at higher energies. Therefore, in order to reduce the influence of yield data in the threshold regime on the entire fit, data at energies below the threshold energy from Eq. (9) were not taken into account for fitting. This demonstrates that the threshold terms in Eqs. (1) and (8) do not correctly describe the threshold behaviour. At the time when Eq. (1) was introduced nearly no data near the threshold energy for sputtering were available. Actually, some efforts are made for a better understanding of the threshold behaviour [13] but, because of the dependence of E_{th} on the mass ratio and angle of incidence, the Ansatz by Bohdansky in Eq. (1) is kept.

The second step for an improvement of Eq. (1) is to find an analytic expression for the fit parameter Q and a better description of E_{th} based on Eq. (8) and the large number of collected data. In order to obtain an analytic scaling of the resulting value Q with the projectile/target parameters, we start from Sigmund's formula (Eq. (2.3.7) in Ref. [14]) for the sputtering yield Y

$$Y = \Lambda F_D, \tag{10}$$

where F_D is the deposited energy and Λ a constant. Assuming power potentials of the form [14]

$$V(r) \propto r^{-1/m}, \quad m \le 1, \tag{11}$$

the values of Λ and F_D can be written

$$\Lambda = \frac{\Gamma_m}{8(1-2m)} \frac{1}{NC_m E_s^{1-2m}},$$

$$F_D = \alpha_s N S_n(E_0) = \alpha_s N 4\pi a_L Z_1 Z_2 e^2 \frac{M_1}{M_1+M_2} s_n(\epsilon). \tag{12}$$

N is the atomic density of the solid and α_s is a dimensionless function of the mass ratio M_2/M_1 and the angle of incidence [2,14]. $NS_n(E_0)$ is the nuclear stopping power. The other values appearing in Eq. (12) are given by the following formulae

$$\Gamma_m = \frac{m}{\psi(1) - \psi(1-m)}, \tag{13}$$

$$C_m = \frac{\pi}{2}\lambda_m a_L^2 \left(\frac{M_1}{M_2}\right)^m \left(\frac{2Z_1Z_2e^2}{a_L}\right)^{2m}. \tag{14}$$

λ_m is a dimensionless function of the parameter m which varies slowly from $m = 1$ at high energies down to $m \approx 0$ at very low energies [14]. a_L is given in Eq. (3), $\psi(x)$ is the digamma function which is defined by

$$\psi(x) = \frac{\mathrm{d} \ln \Gamma(x)}{\mathrm{d}x} = \Gamma'(x)/\Gamma(x). \tag{15}$$

Introducing Eq. (14) into Eq. (12) and Eq. (12) into Eq. (10) leads to

$$Y_m = \frac{\Gamma_m e^{2(1-2m)} \left(\frac{9\pi^2}{128}\right)^{1/3(-1+2m)} \alpha_B^{-1+2m}}{2^{2m}(1-2m)\lambda_m} E_s^{2m-1} (Z_1Z_2)^{1-2m} \left(Z_1^{2/3} + Z_2^{2/3}\right)^{1/2-m} \frac{M_1^{1-m}M_2^m}{M_1+M_2} \alpha_s s_n(\epsilon)$$

$$= q_m E_s^{2m-1} f_m(Z_1, Z_2, M_1, M_2) \alpha_s s_n(\epsilon), \tag{16}$$

where q_m is a constant. Here the term Y_m instead of Y is chosen to demonstrate the dependence of the theoretical sputtering yield on the interaction potential parameter m. One can try to compare Y_m given in Eq. (16) with the yield Y of the revised Bohdansky formula (8) neglecting the threshold terms, i.e. $Y_m = Qs_n(\epsilon)$ and one obtains

$$q_m E_s^{2m-1} f_m \alpha_s = Q. \tag{17}$$

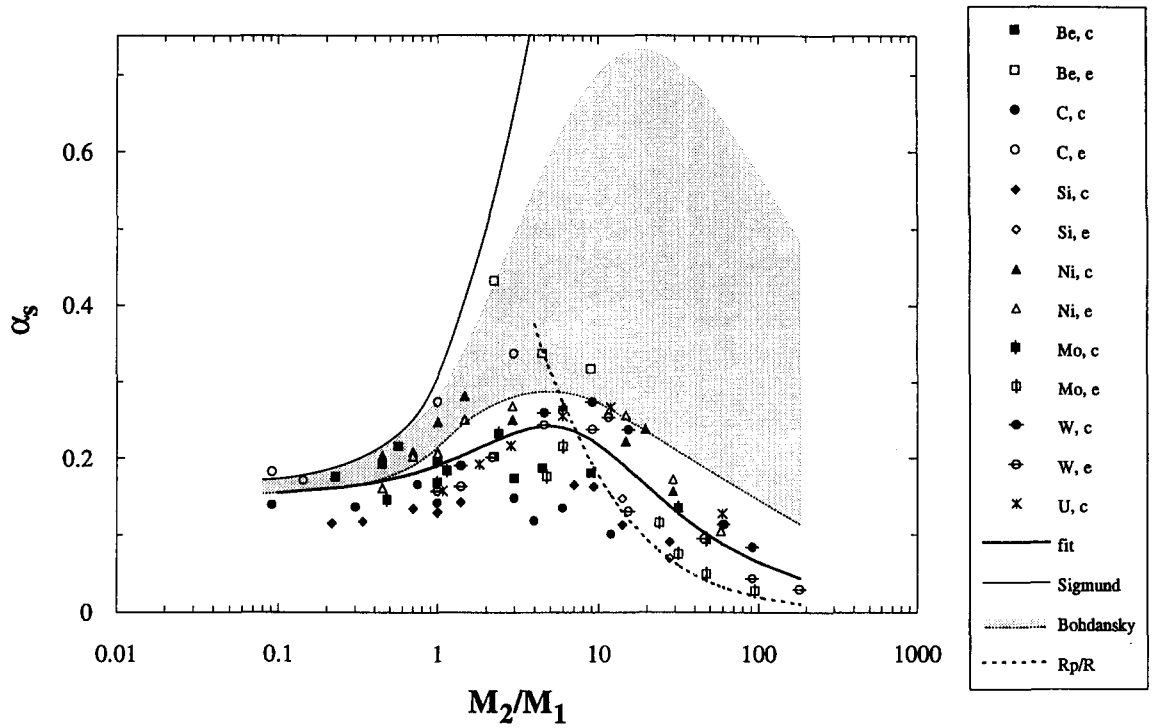

Fig. 3. The value α_s (see text) versus the ratio of target to projectile mass. Solid symbols represent calculated data (c), open symbols experimental data (e). The thin solid line is Sigmund's theoretical curve [13], the thick solid line is the best fit to the data, the dashed curve is the value of R_p/R given by Gott [16]. The shaded area shows the spreading of the α_s values given by Bohdansky in Ref. [2]; the lower limit of the shaded area represents the formula given in the same publication.

Assuming α_s to be a constant, a linear relation between QE_s^{1-2m} and f_m could best be achieved by using $m = 1/6$ which was shown earlier [15,9] to give the best agreement with data from simulations. The value $m = 0$, which corresponds to hard spheres, gives no reasonable fit. Applying $m = 1/6$ changes Eqs. (16) and (17) to

$$QE_s^{2/3} = q_{1/6}\alpha_s f_{1/6}(Z_1, Z_2, M_1, M_2), \tag{18}$$

where

$$q_{1/6} = \frac{\Gamma_{1/6}(e^2)^{2/3}0.8853^{-2/3}a_B^{-2/3}}{2^{1/3}\frac{2}{3}\lambda_{1/6}}, \tag{19}$$

$$f_{1/6} = Z_1^{2/3}Z_2^{2/3}\left(Z_1^{2/3}+Z_2^{2/3}\right)^{1/3}\frac{M_1^{5/6}M_2^{1/6}}{M_1+M_2}. \tag{20}$$

a_B is the Bohr radius and $\lambda_{1/6}$ is determined by interpolation of known values for several m [14],

$$\alpha_B = 0.529\ \mathring{A}, \qquad \Gamma_{1/6} = 0.531, \qquad \text{and } \lambda_{1/6} = 3.8. \tag{21}$$

Introducing Eq. (20) in Eq. (18) results in a value of $q_{1/6} = 1.633$. In Ref. [4] α_s was used as a constant with a fitted value of 0.17 leading to $q_{1/6}\alpha_s = 0.278$; systematic deviations from a linear relationship given in Eq. (17) are thought to be a consequence of the constant value of α_s. However, the dimensionless parameter α_s is a function of the mass ratio M_2/M_1. It can be determined from the experimental and calculated Q values using Eq. (18) and the known charges Z_i and masses M_i of projectiles and targets. The dependence of α_s on the mass ratio M_2/M_1 is shown in Fig. 3. A best fit for α_s is achieved with the formula

$$\alpha_s = \frac{0.15 + 0.05M_2/M_1}{1 + 0.05(M_2/M_1)^{1.6}}, \tag{22}$$

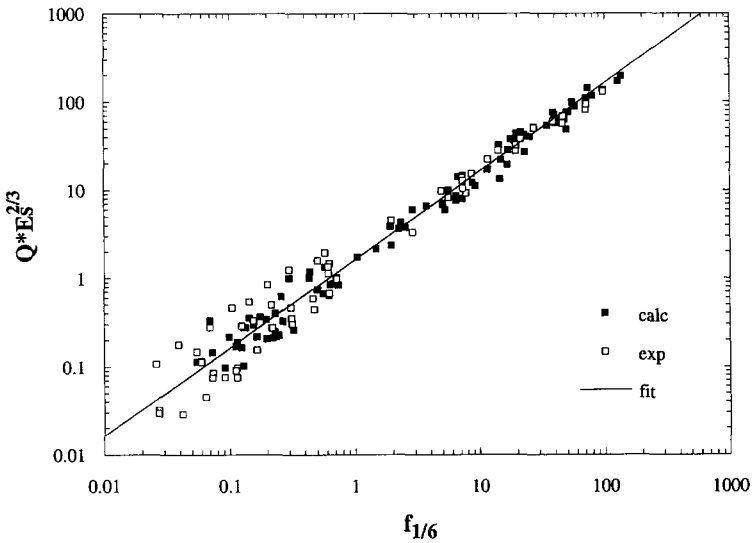

Fig. 4. The value $QE_s^{2/3}$ versus $f_{1/6}\alpha_s$, see Eqs. (18) and (20). Solid squares represent calculated data, open squares experimental data. The solid line is given by Eq. (23).

as shown also in Fig. 3. Eq. (18) can, therefore, be written

$$QE_s^{2/3} = 1.633 Z_1^{2/3} Z_2^{2/3} \left(Z_1^{2/3} + Z_2^{2/3}\right)^{1/3} \frac{M_1^{5/6} M_2^{1/6}}{M_1 + M_2} \frac{0.15 + 0.05 M_2/M_1}{1 + 0.05 (M_2/M_1)^{1.6}}. \tag{23}$$

Eq. (23) leads to a good fit of the experimental and calculated Q values with the predicted charge and mass dependence, see Fig. 4. Especially, at low values of $f_{1/6}$ this procedure gives a better fit than Fig. 141 in Ref. [4] as expected.

In Fig. 3 Sigmund's theoretically predicted α_s is also included. As shown in Fig. 3 the choice for α_s in Eq. (22) is in good agreement with Sigmund's value [13] only at low mass ratios. For large mass ratios Bohdansky [2] gave an analytic expression for α_s based on the ratio of the projected range R_p to the total range (path length) R. Bohdansky's formula, also shown in Fig. 3, seems still too high at large mass ratios. Gott derived the following formula [16]

$$\alpha_s = \frac{R_p}{R} = \frac{4 + 6 M_2/M_1}{3(1 + M_2/M_1)^2}, \quad M_2/M_1 \geq 4, \tag{24}$$

based on the work of Lindhard et al. [17]. Eq. (24) shows too low values at large mass ratios but it should be mentioned that Eq. (24) neglects inelastic energy losses. Eq. (22) gives an empirical fit to the total mass ratio range.

The measured values of α_s given by Bohdansky in Ref. [2] show a stronger spreading as the values given here. This spreading is shown in Fig. 3 by the shaded area and is due to the fact that Bohdansky's α_s is calculated for $m = 0$ in Eq. (16); it should also be mentioned that Bohdansky used the Born–Mayer screening length $a_{BM} = 0.219$ Å [18] independent of Z for the calculation of q_0 ($m = 0$) in Eq. (16) (while for $S_n(E)$ the Lindhard screening length a_L, see Eq. (4), was used which depends on Z_1 and Z_2), leading to a stronger variation of α_s with Z.

The large number of values of the threshold energy E_{th} obtained by fitting experimental and calculated sputtering yields with the revised Bohdansky formula (8) gives the possibility to introduce a better scaling of the threshold energy with the mass ratio. The best fit is achieved with the formula

$$\frac{E_{th}}{E_s} = b_1 \left(\frac{M_2}{M_1}\right)^{b_2} + b_3 \left(\frac{M_2}{M_1}\right)^{b_4} \quad \text{with} \quad b_1 = 7.0,\ b_2 = -0.54,\ b_3 = 0.15,\ b_4 = 1.12, \tag{25}$$

see Fig. 5. Earlier fits vary somewhat but give similar results. It should be remembered that these data are only valid for normal incidence, and that the fit values Q and E_{th} depend on the analytic formula (8) for the energy dependence chosen for the fitting procedure. Besides, calculated values at very low energies had to be omitted for the fitting procedure.

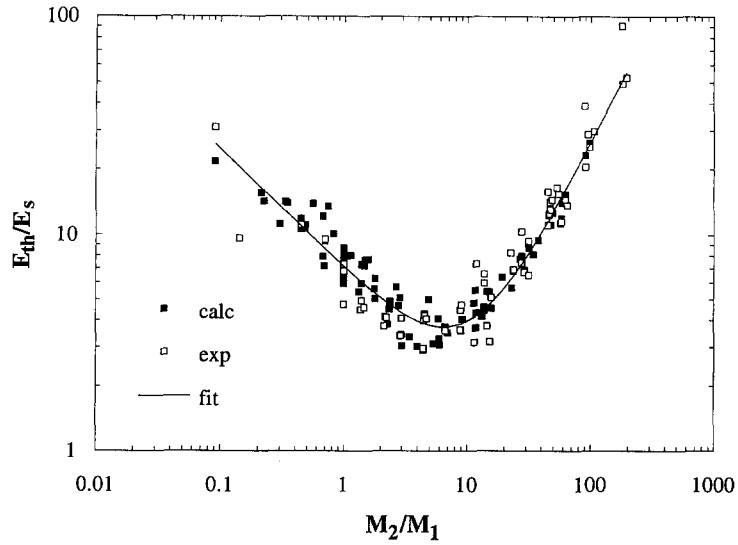

Fig. 5. The relative threshold energy, E_{th}/E_s, versus the ratio of target to projectile mass. Solid squares represent calculated data, open squares experimental data. The solid line, given by Eq. (25), is a fit to all available data.

The fit formulae (23) and (25) give a good guess for the values of Q and E_{th} used in the revised Bohdansky formula (8) as shown in Figs. 4 and 5. Nevertheless, in cases where data are available it is preferable to use the specific fit values given in the figures of the report [4].

The universal Eq. (16) can also be used to make quick estimates of the sputtering yield of different projectile–target combinations. Neglecting the threshold terms the sputtering yield has a maximum where $s_n(\varepsilon)$ has a maximum. This occurs at about $\varepsilon = 0.3$, see Fig. 1. Therefore, the maximum yield is reached at an energy, using Eq. (4),

$$E_0^{max}(\mathrm{eV}) = E_{TF}0.3 = 9.22\frac{M_1+M_2}{M_2}Z_1Z_2\left(Z_1^{2/3}+Z_2^{2/3}\right)^{1/2}. \tag{26}$$

Inserting this energy into the yield Eq. (16) with $m = 1/6$ the maximum possible sputtering yield at normal incidence can be estimated. For light ion sputtering ($M_2 \gg M_1$) and the additional approximation $M_2 \approx 2Z_2$ the yield ratio of different target elements with the indexes (1) and (2) assuming the same projectile becomes

$$\frac{Y_{1/6}^{max}\left(Z_2^{(1)}\right)}{Y_{1/6}^{max}\left(Z_2^{(2)}\right)} = \left(\frac{Z_2^{(2)}}{Z_2^{(1)}}\right)^{1/2}\left(\frac{E_s^{(2)}}{E_s^{(1)}}\right)^{2/3}. \tag{27}$$

For the case of light ion bombardment of W or C this results in a yield ratio of about 4.

Also, the ratio of maximum self-sputtering yields of different materials becomes

$$\frac{Y_{1/6}^{max}\left(Z^{(1)}\right)}{Y_{1/6}^{max}\left(Z^{(2)}\right)} = \left(\frac{Z^{(1)}}{Z^{(2)}}\right)^{14/9}\left(\frac{E_s^{(2)}}{E_s^{(1)}}\right)^{2/3}. \tag{28}$$

This ratio is about 45 for W self-sputtering to C self-sputtering in good agreement with experimental data [4]. For a power potential with $m = 0$, as is often assumed for sputtering, this yield value becomes about 300.

3. Angular dependence of the sputtering yield

The large number of data accumulated for oblique angles of incidence allows us also to check the validity of the available formulae for the angular dependence of the sputtering yield. Yamamura [3] proposed an analytic fit formula for f based on data available at the time

$$f = \sqrt{E_s}\left(0.94 - 1.33\times 10^{-3}M_2/M_1\right). \tag{29}$$

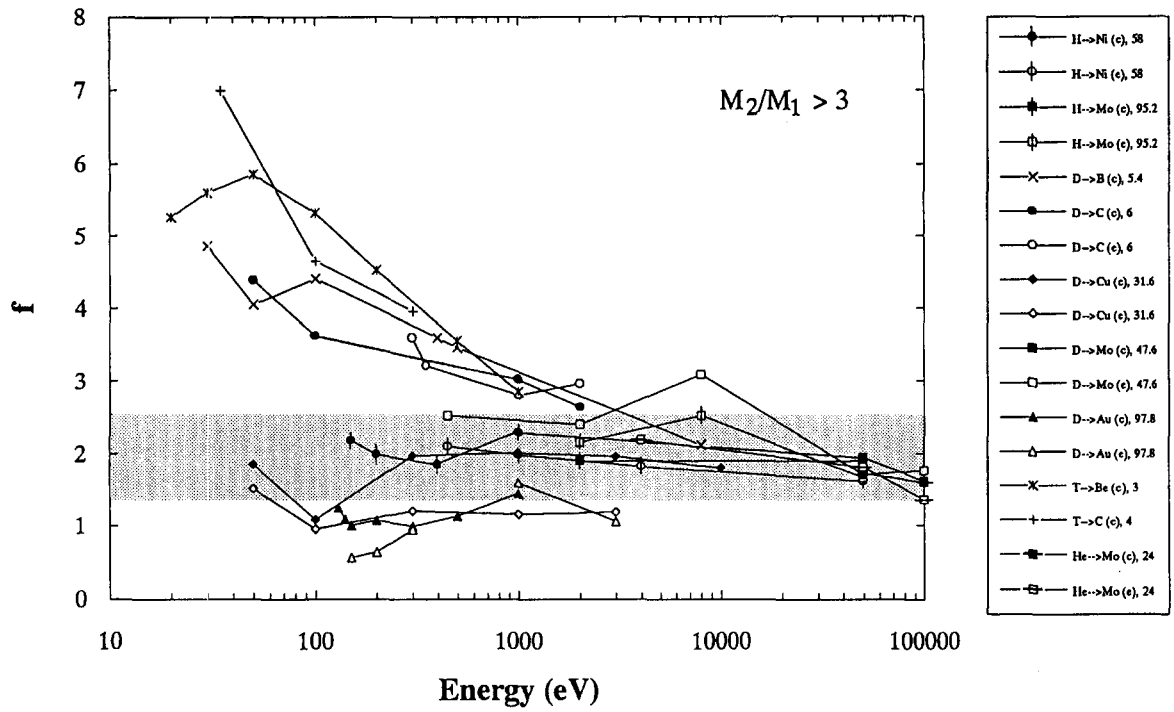

Fig. 6. Fit-values for the fit parameter f of the Yamamura formula (5) versus the projectile energy for target to projectile mass ratios larger than 3. Solid symbols represent calculated data (c), open symbols experimental data (e). Points for the same projectile–target combination are connected by straight lines. The shaded area gives the range of f-values due to Eq. (29) for the projectile–target combinations shown to the right of the figure.

Theoretical considerations [3] led to the following analytic expression for α_{opt}

$$\alpha_{opt} = \pi/2 - a_L n^{1/3}\left(2\varepsilon\sqrt{E_s/\gamma E_0}\right)^{-1/2}, \tag{30}$$

where n is the density of the target material (in atoms/Å^3). As the yield at normal incidence is fixed, uncertainties in $Y(E_0, 0)$ enter the fitting procedure for $Y(E_0, \alpha)$ strongly. We used Yamamura's formula (5) for fitting available yield data measured and calculated at IPP as a function of the angle of incidence for a given energy E_0 [4]. The obtained fit parameters f and α_{opt} are used to check Eqs. (29) and (30). Before, the limitations of formula (5) are discussed.

Yamamura's formula (5) relies on the assumption that the threshold energy is independent of the angle of incidence α. This is approximately correct for light projectiles but seems not to be the case for heavy projectiles as shown in Ref. [13]. Therefore, Eq. (5) is not applicable in the threshold regime for sputtering for heavy projectiles and especially in the case of self-sputtering, where the angle of incidence is limited due to the surface binding potential.

Yamamura's proposed fit for f, see Eq. (29), exhibits a linear relation between $f/\sqrt{E_s}$ and the mass ratio M_2/M_1. Our collected data for f obtained as fit parameter with Eq. (5) agree with Eq. (29) for large mass ratios, but at low mass ratios we observe strong deviations which scale from the ion energy. Therefore we prefer to plot f as a function of the ion energy for different ion/target combinations in order to facilitate reading off the value of f for a given mass ratio and a given energy. This plot is shown in Fig. 6. The shaded area gives the range of f-values due to Yamamura's fit formula (29) for the plotted ion/target combinations.

Yamamura's formula for α_{opt} (Eq. (30)) fits our data for α_{opt} obtained with Eq. (5) only well for light projectiles ($M_2/M_1 > 3$) and not too low energies, but for heavy projectiles and self-sputtering as well as for ion energies near the threshold we observe systematic deviations. Figs. 7 and 8 show α_{opt} as a function of the ion energy for light projectiles ($M_2/M_1 > 3$) and self-sputtering, respectively. In Fig. 8 (self-sputtering) the values for α_{opt} are taken directly from the data points due to the unsatisfying fit with Eq. (5). For large mass ratios α_{opt} agrees with Yamamura's formula (30) at high ion energies, as can be seen in Fig. 7. The shaded area gives the range of α_{opt}

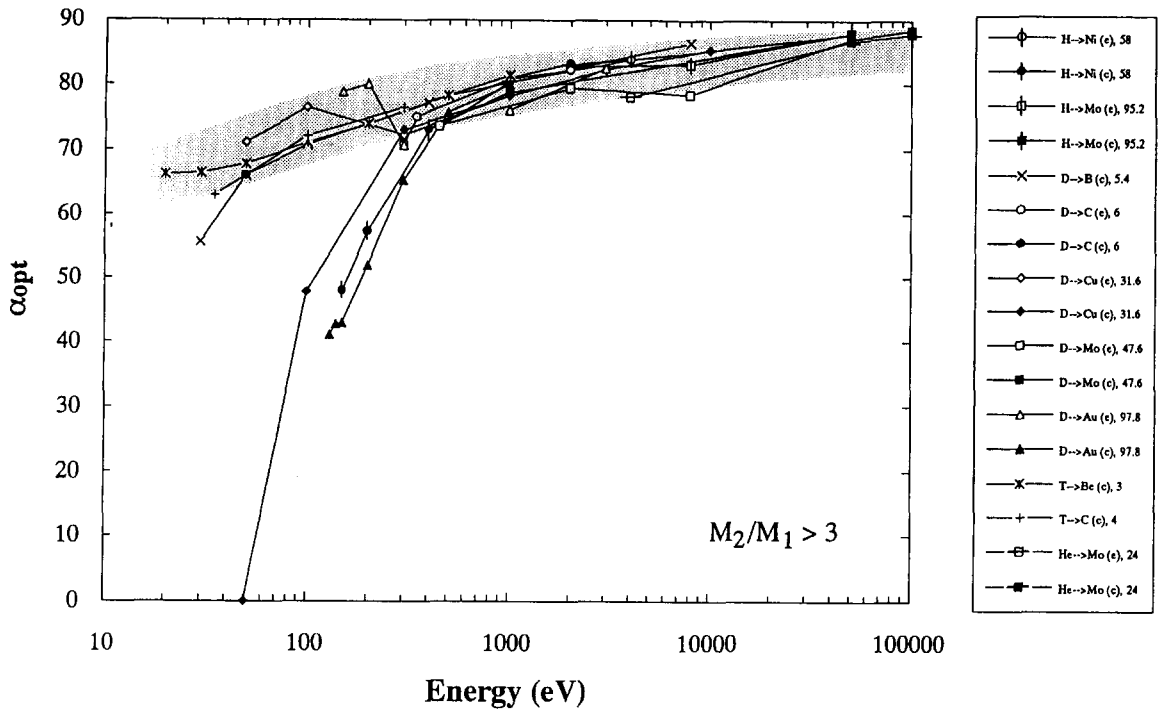

Fig. 7. Fit-values for the fit parameter α_{opt} of the Yamamura formula (5) versus the projectile energy for target to projectile mass ratios larger than 3. Solid symbols represent calculated data (c), open symbols experimental data (e). Points for the same projectile–target combination are connected by straight lines. The shaded area gives the range of α_{opt} values due to Eq. (30) for the projectile–target combinations shown to the right of the figure.

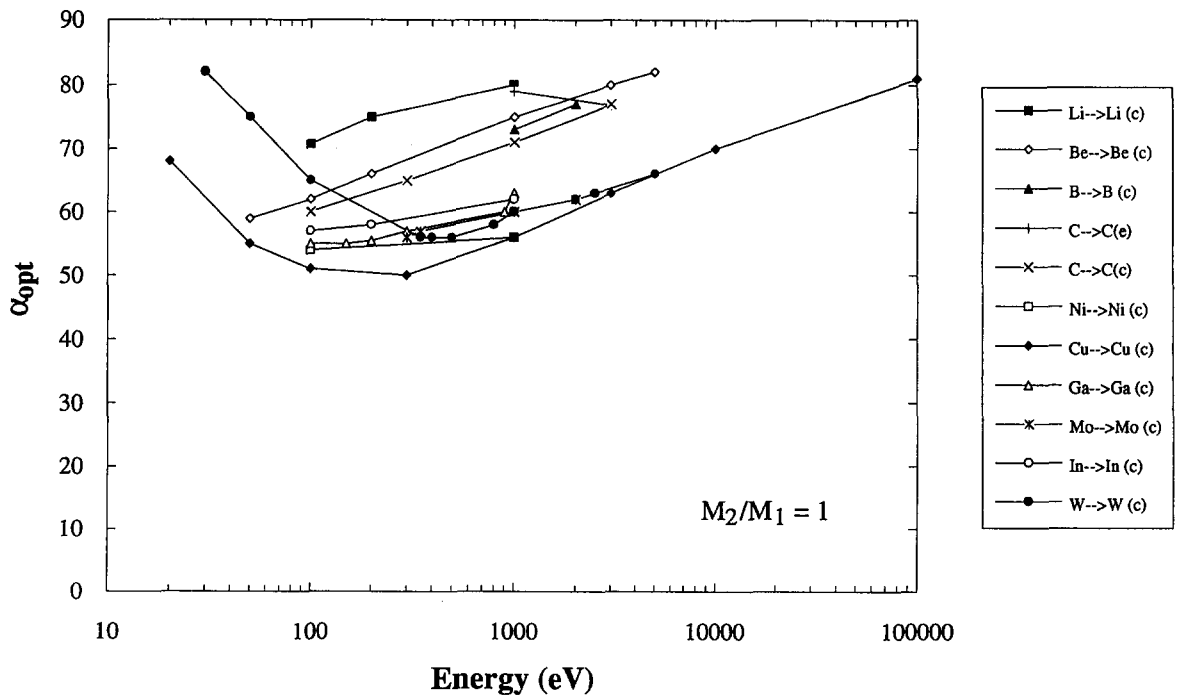

Fig. 8. Fit-values for the fit parameter α_{opt} of the Yamamura formula (5) versus the projectile energy for self-ion bombardment (mass ratio equal to 1). Solid symbols represent calculated data (c), open symbols experimental data (e). Points for the same projectile–target combination are connected by straight lines.

values due to formula (30) for the plotted ion/target combinations. At ion energies near the threshold α_{opt} becomes smaller and it may even reach zero. For low mass ratios and self-sputtering (Fig. 8), on the contrary, the values of α_{opt} at energies near the threshold have a tendency to become larger. This behaviour can be understood considering that, especially for self-sputtering, chemical binding forces at the surface cause an acceleration and a refraction for projectiles leading to a change in the angle of incidence [19]. This effect is negligible for ion energies much higher than the binding forces but it will be of importance in the threshold regime. The values of α_{opt} for self-sputtering and low energies for which Yamamura's formula (5) does not apply can be taken from the lines given by the data points.

4. Conclusions

The large number of measured and calculated sputtering yield data accumulated in the last three decades at IPP allowed the revision and improvement of analytic fit formulae to describe sputtering yields. The Bohdansky formula for calculating sputtering yields as a function of the projectile energy at normal incidence was modified by replacing the nuclear stopping cross-section based on an analytic fit to the Thomas–Fermi potential by one based on the Kr–C potential which results in a better fit of the sputtering data especially at low incident energies. The Bohdansky formula uses two fit parameters, the threshold energy for sputtering, E_{th}, and the parameter Q, which determines the maximum of the yield curve. The large number of fitting values obtained for Q and E_{th} based on the large number of experimental and calculated sputtering yield data allowed also the derivation of analytic expressions for Q and E_{th}. The scaling formula for Q is based on Sigmund's theory for sputtering. The formula for E_{th} is an empirical scaling with the mass ratio. Furthermore, simple formulae for the ratio of the sputtering yields of different targets for the same projectile are given for some limiting cases.

The validity of the formula for the angular dependence of the sputtering yield given by Yamamura has also been checked. It appears that Yamamura's formula is not correct for self-sputtering and for heavy projectiles at energies near the threshold. For not too low energies, i.e. above 1 keV, Yamamura's procedure is acceptable.

References

[1] P. Sigmund, Phys. Rev. 184 (1969) 383.
[2] J. Bohdansky, Nucl. Instr. and Meth. B 2 (1984) 587.
[3] Y. Yamamura, Y. Itikawa and N. Itoh, IPPJ-AM-26, Nagoya (1983).
[4] W. Eckstein, C. García-Rosales, J. Roth and W. Ottenberger, Sputtering Data, Max-Planck-Institut für Plasmaphysik, Report IPP 9/82 (1993).
[5] J. Roth, J. Bohdansky and W. Ottenberger, Data on Low Energy Light Ion Sputtering, Max-Planck-Institut für Plasmaphysik, Report IPP 9/26 (1979).
[6] L.H. Thomas, Proc. Cambridge Philos. Soc. 23 (1927) 542.
[7] E. Fermi, Z. Phys. 48 (1928) 73.
[8] N. Matsunami, Y. Yamamura, Y. Itikawa, N. Itoh, Y. Kazumata, S. Miyagawa, K. Morita and R. Shimizu, Radiat. Eff. Lett. 57 (1980) 15.
[9] J.P. Biersack and W. Eckstein, Appl. Phys. A 34 (1984) 73.
[10] W.D. Wilson, L.G. Haggmark and J.P. Biersack, Phys. Rev. B 15 (1977) 2458.
[11] J.F. Ziegler, J.P. Biersack and U. Littmark, The Stopping and Range of Ions in Solids, The Stopping and Ranges of Ions in Matter, vol. 1 (Pergamon, New York, 1985).
[12] J. Bohdansky, J. Roth and H. Bay, J. Appl. Phys. 51 (1980) 2861 and 52 (1981) 1610.
[13] W. Eckstein, C. García-Rosales, J. Roth and J. László, Nucl. Instr. and Meth. B 83 (1993) 95.
[14] P. Sigmund, Sputtering by Particle Bombardment I, Topics in Applied Physics, vol. 47 (Springer, Berlin, Heidelberg, 1981).
[15] M.T. Robinson, J. Appl. Phys. 54 (1983) 2650.
[16] Yu.V. Gott, Interaction of Particles with Solids in Plasma Investigations (Atomisdat, Moscow, 1978).
[17] J. Lindhard, M. Scharff and H.E. Schiøtt, K. Dan. Vidensk. Selsk. Mat.-Fys. Medd. 33 (14) (1963).
[18] H.H. Andersen and P. Sigmund, Nucl. Instr. and Meth. 38 (1965) 238.
[19] W. Eckstein, Computer Simulation of Ion–Solid Interaction, Springer Series in Materials Science, vol. 10 (Springer, Berlin, Heidelberg, 1991).